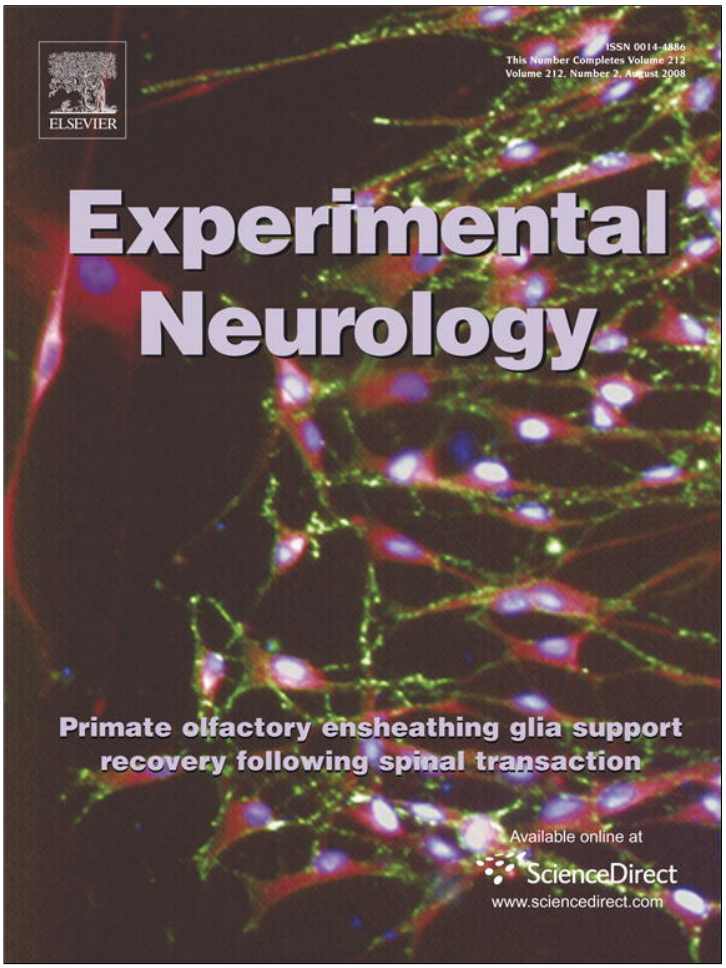

Experimental Neurology 212 (2008) 482–489

Contents lists available at ScienceDirect

Experimental Neurology

journal homepage: www.elsevier.com/locate/yexnr

Dorsal root compression produces myelinated axonal degeneration near the biomechanical thresholds for mechanical behavioral hypersensitivity ☆

Raymond D. Hubbard, Beth A. Winkelstein *

Department of Bioengineering, University of Pennsylvania, Philadelphia, PA 19104, USA

ARTICLE INFO

Article history:
Received 7 December 2007
Revised 24 April 2008
Accepted 28 April 2008
Available online 17 May 2008

Keywords:
Nerve root
Cervical
Degeneration
Radiculopathy
Inflammation

ABSTRACT

Increased sensitivity to mechanical stimuli produced by transient cervical nerve root compression is dependent on the severity of applied load. In addition, trauma in the nervous system induces local inflammation, Wallerian degeneration, and a host of other degenerative processes leading to axonal dysfunction. Here, axonal degeneration and inflammation were assessed following transient dorsal root compression to establish a relationship between conditions for dorsal root axonal changes and those previously established for the onset and maintenance of mechanical behavioral hypersensitivity (26.3 mN and 38.2 mN, respectively). Compression loads were applied over a range (0–110 mN) known to produce sustained behavioral hypersensitivity. CD68- and NF200-immunoreactivity, as well as axonal pathological changes, were assessed in the dorsal root to investigate the load thresholds requisite for inducing macrophage infiltration and axonal degeneration relative to those thresholds for producing the onset and persistence of behavioral hypersensitivity. Neurofilament accumulation and the depletion of NF200-immunoreactivity in the region of compressed tissue were produced for loads that produce mechanical behavioral hypersensitivity. A 50th-percentile load threshold was determined (31.6 mN) governing the onset of NF200 depletion. However, CD68-immunoreactivity was increased for nearly all loads, suggesting that macrophage recruitment may not be directly related to nerve root-mediated behavioral hypersensitivity. This study provides new evidence for threshold-mediated degenerative changes in the context of behavioral hypersensitivity following nerve root compression.

Introduction

Chronic neck pain affects between 30% and 71% of adults at some point during their lives (Côté et al., 1998, 2000; Freeman et al., 1999). Debilitating chronic pain can persist long after a transient injury, resulting in annual societal costs over $29 billion (Freeman et al., 1999). Cervical nerve roots are susceptible to compression injuries because the surrounding bones can change the shape of the intervertebral foramen during neck extension, compression, or especially during complicated combined motions (Nuckley et al., 2002).

Following nerve root trauma, axonal changes indicative of dysfunction and degeneration develop, which depend on the specific mechanical inputs of tissue loading (Olmarker et al., 1989; Kobayashi et al., 1993, 2004; Colburn et al., 1997, 1999; Hashizume et al., 2000; Kobayashi and Yoshizawa, 2002; Sekiguchi et al., 2004; Chung et al., 2005; Singh et al., 2006). Nerve root compression produces endoneurial edema, membrane leakage, and Wallerian degeneration (Olmarker et al., 1989; Kobayashi et al., 1993, 2004; Colburn et al., 1997, 1999; Hashizume et al., 2000; Kobayashi and Yoshizawa, 2002; Sekiguchi et al., 2004). In a canine model, transient compression of lumbar roots for 1 hour using a microvascular clip can produce endoneurial edema in the compressed region as early as 1 hour after the removal of the clip (Kobayashi et al., 1993; Kobayashi and Yoshizawa, 2002). Further, those authors showed that chronic compression produced significant Wallerian degeneration and macrophage recruitment evident at 1 week that were both sustained for at least 3 weeks (Kobayashi et al., 2004).

In response to axonal degeneration, macrophages infiltrate and phagocytize myelin debris, in addition to inducing the release of pro-inflammatory cytokines, including IL-1 and TNF-α (Kobayashi et al., 2004). Axonal degeneration and inflammation can lead to increased electrical activity in adjacent intact axons, and can result in persistent allodynia-like behavioral hypersensitivity (Li et al., 2000; Obata et al., 2003). Axonal injury can also produce a breakdown in fast axonal transport, producing accumulations of transported proteins such as neurofilament (NF) and β-amyloid precursor protein (βAPP) (Chen et al., 1999; Chung et al., 2005; Singh et al., 2006). In fact, βAPP accumulation increases as early as 3–4 hours after injury in a rat model

☆ This work was funded by grant support from the National Institute of Arthritis, Musculoskeletal, and Skin Diseases (#AR047564-02), the Catharine Sharpe Foundation, and fellowship funding from the National Science Foundation.

* Corresponding author. Departments of Bioengineering and Neurosurgery, University of Pennsylvania, 240 Skirkanich Hall, 210 South 33rd Street, Philadelphia, PA 19104-6321, USA. Fax: +1 215 573 2071.
E-mail address: winkelst@seas.upenn.edu (B.A. Winkelstein).

0014-4886/$ – see front matter © 2008 Elsevier Inc. All rights reserved.
doi:10.1016/j.expneurol.2008.04.042

of lumbar nerve root stretch; βAPP accumulation increases with both applied tissue strain and strain rate (Singh et al., 2006). While the results of those studies relate injury mechanics and axonal dysfunction, no studies to date integrate indicators of pathological changes with behavioral assessment to interpret the symptomatic effect of such local pathological changes following mechanical loading.

The severity of nerve root compression modulates behavioral hypersensitivity; yet, while this relationship has been demonstrated in models of painful radiculopathy, applied mechanics have not been well-controlled. Suture ligation of rat lumbar nerve roots was used to establish a relationship between applied tissue strain and mechanical allodynia (pain due to a stimulus that does not normally provoke pain). However, assessments of deformation in that work were made only at the start of the study when the ligation was imposed, and it was assumed that the deformation induced by the ligation remained constant throughout the study (Winkelstein et al., 2001, 2002; Winkelstein and DeLeo, 2002, 2004). Furthermore, those studies focused on spinal cytokine and glial expression and did not identify or characterize *local* pathological changes at the compression site. Sekiguchi et al. (2004) used different sizes of silicon inserts placed in the epidural space to apply compression to the rat cauda equina. Although apoptosis in the dorsal root ganglion (DRG) and axonal degeneration of the central process were produced for larger silicon inserts, no behavioral hypersensitivity was produced for any type of tissue compression (Sekiguchi et al., 2004). The absence of behavioral sensitivity observed in that radiculopathy model underscores the necessity of investigating quantifiable nerve root compression mechanics and local degenerative changes under conditions known to produce a range of behavioral outcomes.

No study has simultaneously investigated the behavioral and pathophysiological outcomes following nerve root compression with different mechanical insults. Our lab has recently identified the load thresholds for producing the onset and persistence of mechanical behavioral hypersensitivity following transient compression of the C7 dorsal root in the rat (Hubbard et al., 2008). While that work identified load thresholds for producing behavioral hypersensitivity, the associated pathologic responses in the nerve root were not investigated. Moreover, the relationship between the load threshold for behavioral hypersensitivity and that for producing tissue damage was not examined. Therefore, the goal of the present study is to define macrophage infiltration, neurofilament accumulation, and axonal degenerative pathology in the dorsal root at days 1 and 7 to determine if the same load thresholds exist for producing local inflammation and axonal degeneration as for producing behavioral hypersensitivity. Accordingly, we utilize the previously defined loads for producing the onset (26.3 mN) and maintenance (38.2 mN) of behavioral hypersensitivity on days 1 and 7 to impose dorsal root compression above or below these thresholds. In these studies, macrophage infiltration, dysfunction of axonal flow, and axonal degeneration are qualitatively and quantitatively assessed by CD68 and NF200-immunoreactivity in longitudinal dorsal root sections, as well as by light and transmission electron microscopy (TEM) in axial cross sections.

Materials and methods

Experiments were performed using male Holtzman rats (Harlan Sprague–Dawley, Indianapolis, IN), weighing 250–350 grams at the start of the study, housed with a 12–12 hour light–dark cycle and free access to food and water. All experimental procedures were approved by the University of Pennsylvania Institutional Animal Care and Use Committee.

Transient dorsal root compression

Surgical procedures for C7 dorsal root compression were performed under halothane inhalation anesthesia (4% halothane for induction, 2% for maintenance). Procedures for the application of cervical dorsal root compression have been previously detailed (Hubbard et al., 2008). Briefly, rats were placed in a prone position, and a C6/C7 hemilaminectomy and facetectomy on the right side exposed the spinal cord and C7 nerve roots. The C7 dorsal root was compressed between micro-compression platens (width 0.7 mm) for 15 min approximately 2 mm from the dorsal root entry zone into the spinal cord. A customized, motor-driven loading device applied a range of compression loads (6.9–93.4 mN) for separate rats (n=12; Table 1), spanning above and below the previously established threshold (26.3 mN) for the *onset* of mechanical behavioral hypersensitivity at day 1 (Hubbard et al., 2008). Nerve root tissue was harvested from those rats at day 1 to assess local degenerative and inflammatory changes. In an additional group, the dorsal root was compressed by loads (5.3–97.9 mN; n=14) ranging above and below the threshold (38.2 mN) defined to produce *persistent* mechanical behavioral hypersensitivity at day 7 (Hubbard et al., 2008). In that group, rats were followed for 7 days before nerve root tissue was harvested. Sham procedures with nerve root exposure but no compression of the dorsal root were performed to provide tissue for comparison on both days 1 (n=4) and 7 (n=4).

Mechanical behavioral hypersensitivity assessment

Mechanical behavioral hypersensitivity in the ipsilateral forepaw was assessed prior to compression (baseline) and on the day of tissue harvest for each group of rats (day 1 and day 7) (Lee et al., 2004; Rothman et al., 2005; Hubbard et al., 2008). A single tester performed all behavioral testing for this study and was blinded to the magnitude of applied load. For each session, following 20 min of acclimation, rats were stimulated on the plantar surface of the right forepaw 30 times using a non-nociceptive von Frey filament (4.0 g; Stoelting Co., Wood Dale, IL), and the total number of paw withdrawals was recorded. For

Table 1
Behavioral hypersensitivity and nerve root pathology

	Rat ID	Applied load (mN)	# Paw withdrawals on Day 1	# Paw withdrawals on Day 7	NF200	CD68	CD68 densitometry (% positive pixels)
Day 1	230	sham	3		–	–	0.1%
	231	sham	2		–	–	0.2%
	232	sham	1		–	–	1.0%
	233	sham	4		–	–	0.7%
26.3mN threshold above ←|→ below	236	6.9	2		–	–	1.0%
	235	7.3	4		–	–	0.7%
	234	9.2	0		–	–	0.5%
	237	10.3	3		–	–	0.9%
	261	33.3	3		–	–	1.1%
	262	37.3	9		–	–	1.4%
	263	44.0	6		–	–	0.9%
	264	49.9	5		–	–	1.2%
	248	81.1	7		–	–	0.4%
	238	83.2	4		–	–	3.6%
	240	92.5	4		–	–	0.3%
	239	93.4	7		–	–	6.6%
Day 7	242	sham		2	–	–	0.2%
	243	sham		1	–	–	0.1%
	244	sham		0	–	–	0.0%
	245	sham		1	–	–	0.7%
38.2mN threshold above ←|→ below	195	5.3		1	–	+	10.4%
	220	7.1		2	–	+	20.1%
	219	9.2		3	+	+	10.2%
	221	15.1		4	–	–	1.3%
	217	22.1		2	–	–	4.2%
	218	33.7		1	+	+	20.2%
	200	38.6		3	–	–	0.1%
	199	56.4		4	+	+	27.8%
	214	67.4		5	+	+	10.0%
	194	71.3		2	+	+	17.8%
	196	72.1		3	+	+	2.6%
	215	90.6		5	+	+	31.3%
	216	95.7		1	+	+	9.1%
	212	97.9		4	+	+	19.3%
	246	normal	1	1	–	–	0.3%
	247	normal	0	0	–	–	1.7%

+ indicates axonal swellings and decreased NF200-immunoreactivity, or increased CD68-immunoreactivity.
– indicates no abnormal pathology.

each day, rats were separated into groups based on whether they received compression *above* or *below* the threshold for that day (i.e. relative to 26.3 mN or 38.2 mN, respectively). For each time point, mechanical behavioral hypersensitivity for the groups *above-threshold* and *below-threshold* were compared to the number of sham paw withdrawals using a one-way analysis of variance with post-hoc Bonferroni correction. Statistical analyses were performed using SYSTAT v10.2 (Richmond, CA), with significance at $p<0.05$.

Macrophage infiltration and axonal degeneration

Macrophage infiltration, neurofilament accumulation, and loss of myelinated axons were assessed in the dorsal roots on each of days 1 and 7 after compression, in separate studies. An overdose of sodium pentobarbital (40 mg/kg) was given, and rats were transcardially perfused with 150 ml of phosphate buffered saline (PBS) followed by 150 ml of 4% paraformaldehyde in PBS. The C7 nerve roots were harvested and paraffin embedded for immunohistochemical analyses. Nerve roots from normal, naïve rats ($n=2$) were also processed as controls to account for tissue processing effects. Longitudinal nerve root sections (10 μm), which included the full length between the dorsal root entry zone and the DRG, were collected on gelatin-coated slides for each rat. Sections (3–5 per rat) were immunolabeled for infiltrating macrophages or heavy chain neurofilament (NF200) using monoclonal antibodies against the CD68 receptor (ED1, 1:500; Serotec, Kidlington, UK) and phosphorylated and non-phosphorylated NF200 (N52, 1:400; Sigma, St. Louis, MO), respectively. A horse anti-mouse secondary antibody (Vector, Burlingame, CA) was used at a dilution of 1:400 (for CD68) or 1:1000 (for NF200). All antibody dilutions used in this study were previously optimized. Sections were exposed to 3,3-diaminobenzidine (Vector Labs, Burlingame, CA) for color development and cover-slipped using a non-aqueous mounting medium.

NF200-immunoreactivity was visually evaluated in representative longitudinal sections of the dorsal root for the presence of axonal swellings or an excessive decrease in fiber staining. A representative section for each rat was digitally imaged at 100× magnification and evaluated relative to uncompressed nerve roots (Chen et al., 1999). Tissue sections that displayed axonal varicosities or considerably reduced fiber staining were assigned a value of (+); sections not different from uncompressed roots were assigned a grading of (−). Macrophage infiltration in adjacent sections was similarly evaluated in representative sections. Increased CD68-immunoreactivity relative to uncompressed nerve roots was assigned a grade of (+), and little or no increase in immunoreactivity was given a grade of (−). Grading of decreased NF200- or increased CD68-immunoreactivity was fit by logistic regression against the applied load for each marker on days 1 and 7, separately. Significance of the regression was determined by a chi-squared test. The 50th-percentile load value is reported as the threshold for producing a grade of (+) for NF200- or CD68-immunostaining in the nerve root (±95% confidence interval). Tissue sections labeled for CD68-immunoreactive macrophages were also analyzed using densitometry to quantify the area occupied by macrophages within a square region of interest (ROI), with a width equal to that of the dorsal root at the compression region. A customized Matlab (Natick, MA) program counted the number of pixels within the ROI with a gray-scale intensity darker than that of background tissue staining.

To evaluate degenerative pathology relative to the magnitude of applied compression, axons of the compressed (ipsilateral) and uncompressed (contralateral) dorsal root were assayed in cross sections for myelin abnormalities indicative of Wallerian degeneration in a subset of rats ($n=6$). Based on reports that the myelin structure is unchanged at day 1 for a variety of different types of neural traumas (i.e. nerve crush, nerve transection, heat application) (Beirowski et al., 2005; Podhajsky et al., 2005), tissue was analyzed only at day 7. The right C7 dorsal root was compressed by loads (3.0 and 11.4 mN) below 38.2 mN (day 7 threshold), slightly above that threshold (49.3 and 57.8 mN), or sufficiently above that threshold (72.6 and 102.1 mN). On day 7, an overdose of chloral hydrate was given, and rats were transcardially perfused with 50 ml 0.9% saline followed by 50 ml of 2% paraformaldehyde, 2.5% glutaraldehyde in saline. C7 nerve roots were harvested and incubated in 2% OsO_4 in 0.1 M phosphate buffer for 1 h. Samples were then embedded in epon resin.

For light microscopy, five axial semithin sections (0.5 μm) were taken approximately 800 μm from the dorsal root entry zone central to the compression site and stained with toluidine blue for 1 min to enable visualization of myelinated axon caliber and degeneration in the dorsal root central to the compressed region. A neuropathologist reviewed all sections and provided an evaluation of degeneration. One representative section per rat was imaged at 630× magnification. For TEM, five thin sections (0.1 μm) immediately adjacent to the semithin sections were stained with uranyl acetate for 40 min. The entire cross-sectional area of the dorsal root was assessed in each image for the presence of degenerated axons, macrophage phagocytosis of extra-tubal myelin debris, and myelin abnormalities such as incisures or thin or no myelination surrounding medium and large caliber axons. Dorsal roots displaying any of these hallmarks were assigned a grade of (+), while (−) was assigned for no difference from the uncompressed, contralateral dorsal root. Evidence of degeneration was compared for each load group in the context of the 38.2 mN load threshold to produce persistent behavioral hypersensitivity.

Results

Mechanical behavioral hypersensitivity

Mechanical behavioral hypersensitivity at days 1 and 7 exhibited a dependence on load that was consistent with the previously established thresholds (Hubbard et al., 2008). Sham procedures did not produce significant changes in mechanical behavioral hypersensitivity compared to baseline at either time point (Fig. 1). A positive paw withdrawal was often accompanied by a head turn response and/or vocalization, indicating a supraspinal allodynia-like response. On day 1, there was no difference in hypersensitivity relative to sham for compression loads below the 26.3 mN threshold (Fig. 1). However, loads above that mechanical threshold produced hypersensitivity that was significantly elevated over sham ($p=0.04$, Fig. 1). Similarly, at day 7, behavioral hypersensitivity was not produced for applied compressions that were below the corresponding threshold (38.2 mN) for

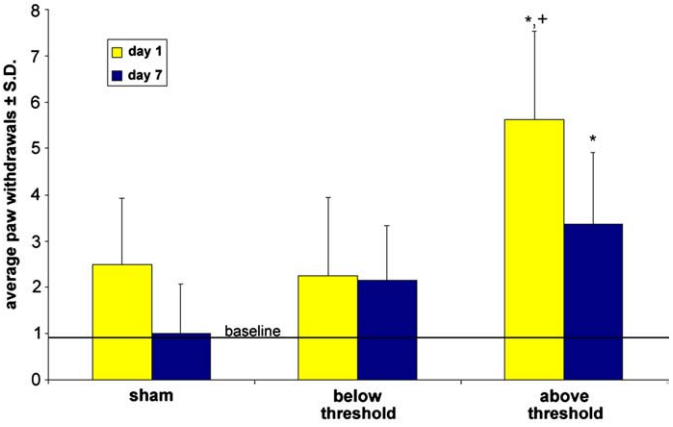

Fig. 1. Ipsilateral mechanical behavioral hypersensitivity for sham, below threshold, and above threshold compression groups on days 1 and 7 using a 4 g von Frey filament. Average responses for each group are reported as the number of forepaw withdrawals (±standard deviation). A significant increase was observed for above threshold groups on both days over sham (*$p<0.05$) and at day 1 over the below threshold group (+$p<0.05$).

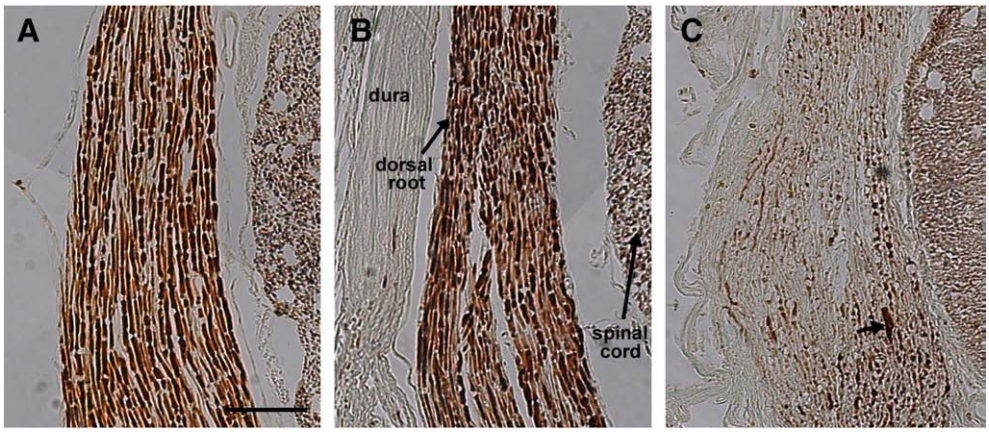

Fig. 2. Representative images within the 700 μm compression region of the C7 dorsal root at day 7 immunostained against NF200. Dorsal roots from the (A) uncompressed and (B) below 38.2 mN groups exhibited long, unbroken axonal staining. (C) Dorsal roots compressed by loads above that threshold for behavioral hypersensitivity exhibit substantial decreases in NF200-immunoreactivity and axonal swellings (arrow). Scale bar in (A)=100 μm and applies to all.

hypersensitivity at that day, but loading above that force did produce behavioral hypersensitivity that was significantly elevated over sham (p=0.02, Fig. 1).

Neurofilament immunoreactivity and macrophage infiltration at day 1

At 1 day after compression, no changes relative to sham or normal responses were observed for NF200-immunoreactivity in compressed nerve roots (Table 1). In addition, there was no increase in macrophage infiltration in any nerve root assessed at day 1 for any compression. As such, logistic regressions for NF200- and CD68-immunoreactivity did not determine a 50th-percentile load value (data not shown). Densitometry measurements reflected minimal detection of CD68-immunoreactivity; only two rats (#238, #239) displayed CD68-immunostaining greater than 3%, and these rats each received loads greater than 80 mN (Table 1).

Neurofilament immunoreactivity at day 7

Changes in neurofilament immunoreactivity were observed in the dorsal root at day 7 following compression and depended on the magnitude of load (Table 1). NF200 immunostaining in the normal, naïve C7 dorsal root revealed long, myelinated axons with an even distribution of staining along their lengths (Fig. 2A). No differences in axonal staining were observed in nerve roots receiving sham procedures compared to normal (Table 1). On day 7 after compression below 38.2 mN, only minimal decreases in NF200-immunoreactivity were observed in the compressed region of roots and no varicosities were observed (Fig. 2B). However, compression by loads greater than 38.2 mN produced a moderate to dramatic decrease in NF200-immunoreactivity relative to sham along the full length of the dorsal root. Axons formed varicosities both proximal and distal to the site of compression that were not seen in dorsal roots from sham rats (Table 1, Fig. 2C). The changes in NF200-immunoreactivity at day 7 were also considerably increased relative to those observed in roots at day 1 compressed by similar magnitudes of load. Logistic regression of NF200 grading at day 7 against compression load predicted a threshold of 31.6 mN (±9.4 mN) to significantly reduce transport of NF200 (p<0.0001; Fig. 3A).

Axonal degeneration at day 7

Wallerian degeneration and myelin breakdown in the dorsal root central to the site of compression increased with the magnitude of applied load (Table 2, Fig. 4). In two of four dorsal roots compressed with loads below or slightly above 38.2 mN, loading produced no axonal abnormalities (Fig. 4B) compared to the uncompressed, contralateral roots (Fig. 4A). For the remaining two roots compressed with loads below or slightly above 38.2 mN, a loss of myelinated axons was observed only in small regions near the perimeter of the cross section. All areas within the central portion of the cross section showed no evidence of degeneration, and the myelinated axons remained tightly packed (Fig. 4B). Loads that were sufficiently above 38.2 mN (#269, #271) produced a considerable loss of myelinated axons in regions both

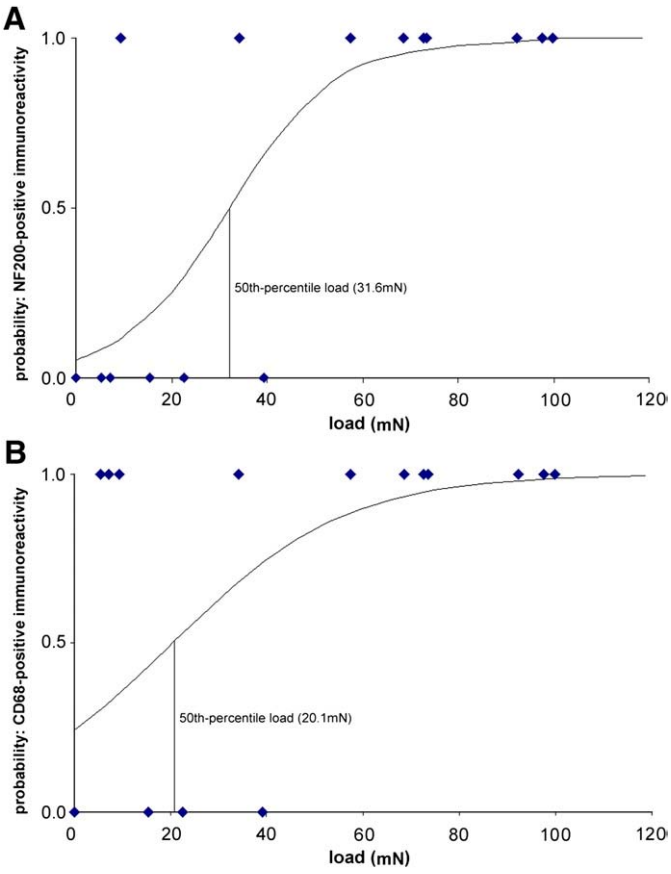

Fig. 3. Logistic regressions for assessment of (A) NF200- and (B) CD68-immunoreactivity at day 7 after dorsal root compression. The 50th-percentile load thresholds for producing axonal pathology or macrophage infiltration are significant and indicated at (A) 31.6 mN and (B) 20.1 mN, respectively.

Table 2
Axonal degeneration

Rat ID	Applied load (mN)	Axonal degeneration
267	3.0	–
272	11.4	+
268	49.3	–
266	57.8	+
269	72.6	+
271	102.1	+

+ indicates myelin degradation and Wallerian degeneration.
– indicates no abnormal pathology.

around the perimeter and within the center of the root cross section (Fig. 4C). Large denervated cellular regions lacking myelinated axons surrounded intact myelinated and unmyelinated axons (Fig. 4C). Occasionally, surviving large diameter axons displayed myelin deformities or incisures. Myelin debris was engulfed by macrophages outside the basal laminae of degenerated axons (Fig. 4D). In some cases, macrophages and Schwann cells containing lipid droplets were observed within the remaining basal lamina of degenerated axons. The existence of unmyelinated and thinly myelinated large caliber axons indicated demyelination and/or regeneration (Fig. 4D). In many cases, several medium diameter axons regenerated within a single Schwann cell basal lamina from a degenerated axon. These significant pathological changes were consistently observed only in tissue undergoing loading sufficiently above 38.2 mN.

Macrophage infiltration at day 7

At day 7, CD68-positive macrophages in the C7 dorsal root were evident for compressions throughout the full range of loads (Table 1). In fact, only three compressed roots did not display any evidence of macrophage infiltration. For normal naïve rats, few macrophages were observed on the dura surrounding the dorsal root, and none were present within the dorsal root (Fig. 5A). No increase in macrophage recruitment above normal was present for shams (Table 1). For all compression loads, at day 7 macrophages penetrated the dura mater, and infiltration was more robust than at day 1 (Table 1, Fig. 5). Immunostaining was concentrated near the site of compression, extending into the DRG; staining extended into the spinal cord for two roots compressed above 38.2 mN (#199, #215) (Fig. 5). For all samples except one (#200) receiving a load above the threshold for producing persistent behavioral hypersensitivity, the root was fully infiltrated by macrophages and myelin debris was engulfed within the macrophages (Fig. 5C). However, most roots loaded below that threshold also demonstrated considerable CD68-immunoreactivity in the perineurium and among the dorsal root fibers (Fig. 5B). By logistic regression, the 50th-percentile load threshold for producing increased macrophage infiltration at day 7 was predicted at 20.1 mN (±10.3 mN). This regression had a significant chi-squared distribution ($p<0.004$) despite positive immunostaining for most sub-threshold compression loads (Table 1, Fig. 3B). The trend in macrophage infiltration across all loads was also detected by quantitative densitometry analysis

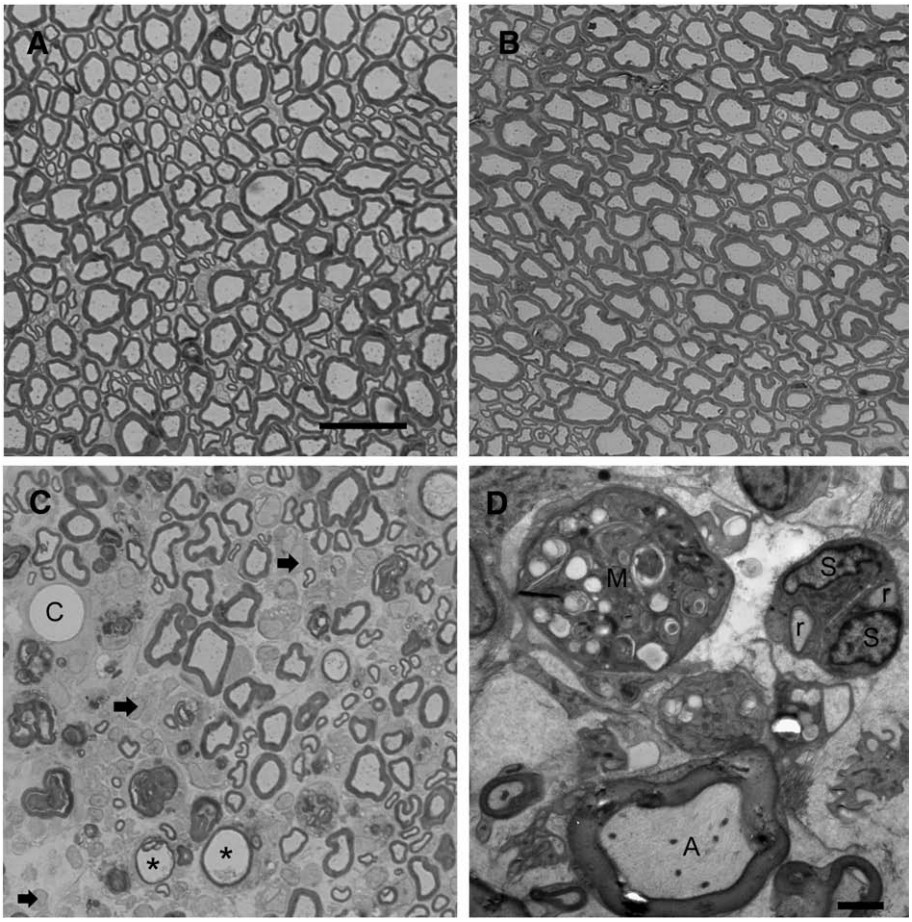

Fig. 4. (A–C) Representative images of axial sections of the C7 dorsal root approximately 800 μm from the dorsal root entry zone, central to the site of compression, stained with toluidine blue at day 7. Images demonstrate samples that underwent (A) no loading, (B) a 49.3 mN load, and (C) a 72.6 mN load. (C) Large denervated cellular regions lacking myelinated axons (arrows) are surrounded by surviving axons. Remaining myelin sheaths from degenerated axons (*) are also present following large loads but not for the smaller loads or unloaded case. A capillary is indicated by the letter 'C'. (D) Transmission electron microscopy image of the same dorsal root compressed by a load of 72.6 mN (C) demonstrates a macrophage (M) engulfing myelin debris near a surviving myelinated axon (A). Regenerating axons (r) surrounded by the basal laminae of Schwann cells (S) are also observed. Scale bar in (A)=20 μm and applies to (A) through (C). Scale bar in (D) =2 μm.

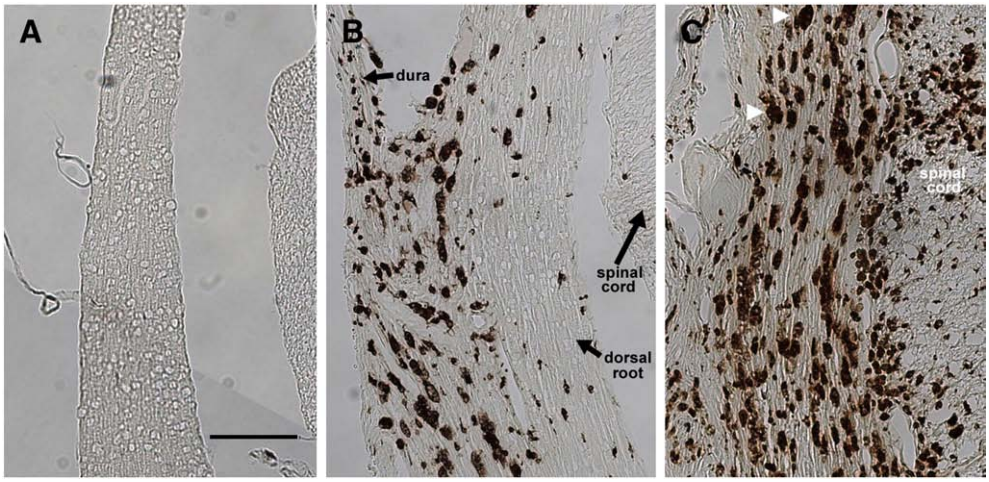

Fig. 5. Representative images of the region of compression at day 7 immunostained against the CD68 receptor. Moderate or high CD68-immunoreactivity was observed in the majority of roots that were compressed, either (B) below or (C) above the threshold for behavioral hypersensitivity. Such reactivity was not apparent in (A) uncompressed roots. (C) Macrophages phagocytizing myelin debris (arrow heads) are present for most compression loads, extending into the spinal cord in some cases. Scale bar in (A) = 100 μm, applies to all.

(Table 1). For all compression loads, there was at least a small increase in macrophage infiltration relative to sham. Immunostaining in greater than 10% of the compression region was observed in most of the samples loaded both above and below 38.2 mN (Table 1).

Discussion

This study demonstrates that transient compression of the cervical dorsal root is sufficient to disrupt proteins used for axonal transport in myelinated fibers within the compressed root for certain magnitudes of load (Table 1, Figs. 2 and 3). Further, the load threshold (31.6 mN) for producing axonal swellings and decreases in NF200-immunoreactivity at day 7 is similar to the threshold previously determined (38.2 mN) for producing mechanical behavioral hypersensitivity at that same time point in this radiculopathy model (Hubbard et al., 2008). Macrophage infiltration is also observed within the compressed roots at this same time point, but does not demonstrate a strong dependence on load magnitude (Table 1, Figs. 3 and 5). Despite behavioral hypersensitivity being produced at day 1 following compression for loads above 26.3 mN (i.e. those cases where load is greater than the threshold for onset of behavioral hypersensitivity), neither NF200- nor CD68-reactivity were observed to be different from the uncompressed root at this time point (Table 1). While assayed in a limited number of samples, myelinated axon degeneration central to the compression site at day 7 generally followed the trends exhibited by NF200, further suggesting that axonal damage and dysfunction are produced by compression loads that correspondingly produce behavioral hypersensitivity.

Immediately following trauma to neural tissue, the initial stages of Wallerian degeneration produce structural defects in myelin, which signal the activation of resident endothelial, immune, and glial cells. These cells release inflammatory cytokines and present chemoattractant molecules, which recruit macrophages to phagocytize the myelin debris (Watkins and Maier, 2002). Infiltrating macrophages also release their own store of cytokines, prostaglandins, and degradative enzymes (Ma and Eisenach, 2003). In this study, mechanical behavioral hypersensitivity was produced at 1 day following dorsal root compression for loads greater than 26.3 mN (Table 1, Fig. 1), prior to the production of detectable changes in NF200- or CD68-immunoreactivity, suggesting no breakdown in axonal architecture or local inflammation at that early time point. However, at day 7 axonal degeneration and macrophage infiltration were evident for loads producing persistent behavioral hypersensitivity (Tables 1 and 2, Figs. 2, 3, 4 and 5). The absence of these same tissue responses at day 1 suggests either that early stages of degeneration and inflammatory signaling are not yet detectable or that the onset of behavioral hypersensitivity is not mediated by local degenerative or inflammatory changes. Vasogenic edema in the nerve root has been shown to increase within 1 h for compression loads greater than 15 gf (147 mN) in a canine model of lumbar radiculopathy (Kobayashi et al., 1993; Kobayashi and Yoshizawa, 2002); although those canine studies did not investigate behavioral outcomes, the enhanced extravasation of protein tracers from radicular capillaries following nerve root compression suggests a potential route for circulating inflammatory cells to infiltrate the endoneurial space. Moreover, inflammatory cytokines, such as TNF-α and IL-1β, can increase in the DRG and spinal cord as early as within the first 24 h in models of neuropathic and inflammatory pain (Cuellar et al., 2004; Sommer and Kress, 2004; Xie et al., 2006). Since macrophage infiltration was not observed at day 1 (Table 1), if the onset of nerve root-mediated behavioral hypersensitivity involves local cytokines, the source of these cytokines may be the resident neurons and/or glial cells already present at the site of injury.

Neurons in the DRG become hyperexcitable immediately after injury to their axons, which can also lead to extended periods of spontaneous ectopic neuronal firing and pain (Sheen and Chung, 1993; Waxman et al., 1999; Boucher et al., 2000; Iwata et al., 2004; Zhang et al., 2004; Kirita et al., 2007). Several studies suggest that ectopic firing after axonal damage results from calcium influx or altered sodium channel subtype expression (Waxman et al., 1999; Boucher et al., 2000; Iwata et al., 2004; Kirita et al., 2007). These changes in ion flux could be responsible for the acute behavioral hypersensitivity produced in the absence of immediate axonal degeneration. Together with the results from this study, such findings suggest that immediate behavioral hypersensitivity in this model of transient compression may result from an immediate release of proinflammatory cytokines by resident cells, or via altered primary afferent electrical activity that occurs prior to the neuronal degeneration or macrophage infiltration observed later at day 7 (Figs. 3 and 5) (Waxman et al., 1999; Boucher et al., 2000; Cuellar et al., 2004; Sommer and Kress, 2004; Iwata et al., 2004; Xie et al., 2006; Kirita et al., 2007). Further studies are required to determine the role of these inflammatory mediators as a function of nerve root compression mechanics.

Data from this study suggest that similar mechanical load thresholds govern degeneration and persistent mechanical behavioral hypersensitivity observed at day 7 (Fig. 3). Both the depletion of NF200-immunoreactivity in the compressed region of the dorsal root and Wallerian degeneration central to the site of compression were load-dependent in this study. In previous studies, markers of

myelinated axonal loss have not been observed immediately, but develop over the first week after compression (Brück, 1997; Kobayashi et al., 2004). Within the first week after neuronal compression, neurons exhibit decreased firing thresholds and increased action potential durations (Ma et al., 2003). During that time frame, the progression of Wallerian degeneration can alter electrophysiology and membrane properties in compressed neurons and increase signaling of leukocytes and chemokines, enhancing neuronal excitability in adjacent, surviving axons (Boucher et al., 2000; Li et al., 2000; Brack and Stein, 2003; Obata et al., 2003; Song et al., 2003; White et al., 2005; Tan et al., 2006). While surviving axons can produce aberrant signals after compression, regenerating A-fibers may also re-map to the superficial laminae of the spinal cord (Ramer et al., 1997; Nakamura and Myers, 1999, 2000; Watanabe et al., 2007). This plasticity provides a potential mechanism by which normal mechanosensation may be interpreted as painful stimuli even after aberrant neuronal firing has decreased. With these neuronal changes associated with the degenerative process occurring at the same loads that cause persistent behavioral hypersensitivity, axonal degeneration may likely contribute to sensitivity consistent with an allodynia-like response. Of course, the possibility remains that degeneration changes may be only correlative with behavioral changes. Dorsal root compression produced a significant decrease in NF200-immunoreactivity at day 7 for loads greater than a 50th-percentile load of 31.6 mN (±9.4 mN), while the load threshold for producing persistent mechanical behavioral hypersensitivity was 38.2 mN (Hubbard et al., 2008). Wallerian degeneration was also present in myelinated axons for large compression loads (Table 2, Fig. 4), confirming that the survival of the compressed axons appears to depend on the mechanical profile of the traumatic insult. While previous studies demonstrate that compression of axons can produce hypersensitivity and degeneration (Myers et al., 1996; Brück, 1997; Sekiguchi et al., 2003), this is the first study to define a load threshold for transient compression above which *both* degenerative pathological changes and behavioral hypersensitivity are produced.

Although this study provides evidence linking axonal degeneration with behavioral symptoms consistent with pain responses following mechanical nerve root trauma, infiltrating macrophages did not exhibit the same degree of sensitivity to applied load. The low load for producing elevated CD68-immunoreactivity (Table 1) suggests that while an inflammatory response may augment the aberrant axonal firing activity associated with allodynia-like responses (Song et al., 2003), macrophage infiltration alone may not be sufficient to produce a behavioral response. CD68-positive macrophages were observed to infiltrate the compressed root at day 7, for even the lowest compression loads (Table 1). The threshold (20.1 ± 10.3 mN) determined for macrophage recruitment at day 7 was lower than that for producing persistent behavioral hypersensitivity (Fig. 3B). It is possible that macrophage infiltration observed here is primarily a result of the perceived disruption of the axonal architecture and myelin sheath (Brück, 1997, Scherer and Salzer, 2001) and is only indirectly associated with behavioral hypersensitivity. Cui et al. (2000) found that neuropathy models that produced the most behavioral hypersensitivity were correlated with those that also produced the greatest macrophage response. However, the variation in hypersensitivity between model types in that study suggests that macrophage infiltration is more sensitive to axotomy or photochemical lesion than to chronic constriction, not that macrophages necessarily affect the development of behavioral hypersensitivity. Additionally, when the ubiquitous macrophage response was suppressed by depleting the peripheral macrophage population in a chronic neuropathy model, Rutkowski et al. (2000) was not able to abolish behavioral hypersensitivity. Taken together with our findings, these studies suggest that macrophage infiltration, in response to perceived axonal damage, may enhance neuronal hyperexcitability, but the macrophage response alone may not elicit behavioral hypersensitivity.

NF200-immunoreactivity is used in this study to infer the damage to all fiber subtypes in the dorsal root. However, NF200 is primarily expressed in large diameter neurons not small, nociceptive afferents. Stone et al. (2004) suggest that impairment of axonal transport following mechanical tissue strain is variable across different sized fiber subpopulations and that such impairment is preferentially more severe in larger axons. That report implies that an assessment of NF200 transport impairment may overestimate the damage that is produced in small, unmyelinated fibers because those fibers are less susceptible to damage following tissue strain. The load threshold (31.6 mN) for producing decreases in NF200 determined here is a mild underestimate of the threshold for persistent mechanical behavioral hypersensitivity (38.2 mN), which corroborates the assertion that NF200-immunoreactivity overestimates damage to nociceptive fibers. The similarity in load thresholds for NF200-immunoreactivity and behavioral hypersensitivity consistent with allodynia-like responses strongly implicates local axonal disruption and degeneration in contributing to persistent pain. Certainly, this study investigated responses at only two time points after nerve root compression, and results should be interpreted in that context. The local and spinal cascades following nerve root injury are multifaceted and temporally dynamic, and findings from this study reflect only those results at days 1 and 7. Additional studies at later time points and with larger sample sizes would enable more detailed insight into the complicated relationships between load, injury, neuronal and inflammatory responses, and behavioral hypersensitivity. Accordingly, the thresholds defined in this study reflect findings incorporating the inherent limitations with time points and sample sizes.

In summary, transient compression of the cervical dorsal root produces load-dependent axonal transport disruption and degeneration on day 7, and the threshold for producing these pathological changes is very similar to that load required to produce sustained behavioral hypersensitivity. In contrast, CD68-immunostaining is evident at day 7 regardless of the production or absence of behavioral symptoms. Despite the presence of behavioral hypersensitivity on day 1, neither neurodegeneration nor macrophage infiltration was observed at that time point, suggesting that aberrant neuronal firing and immediate changes in axonal properties may contribute to the onset of behavioral hypersensitivity. Taken together, these data suggest that load-based Wallerian degeneration and transport interruption are strongly associated with persistent behavioral hypersensitivity. Macrophage infiltration may be a component of the inflammatory response that is only indirectly associated with behavioral hypersensitivity. However, there are likely aspects of the local inflammatory response that specifically contribute to persistent pain (Watkins and Maier, 2002). Nonetheless, the similarity between load thresholds for initiating morphological changes in myelinated axons and mechanical behavioral hypersensitivity in transient root compression suggest that axonal dysfunction, or its sequelae, mediate maintained behavioral hypersensitivity, and, if prevented, may reduce persistent pain.

Acknowledgments

We would like to thank Dr. Steven Scherer and his lab for their scientific and methodological expertise, and for use of his laboratory equipment and TEM for studies investigating Wallerian degeneration.

References

Beirowski, B., Adalbert, R., Wagner, D., Grumme, D.S., Addicks, K., Ribchester, R.R., Coleman, M.P., 2005. The progressive nature of Wallerian degeneration in wild-type and slow Wallerian degeneration (WldS) nerves. BMC Neurosci. 6, 6.

Boucher, T.J., Okuse, K., Bennett, D.L., Munson, J.B., Wood, J.N., McMahon, S.B., 2000. Potent analgesic effects of GDNF in neuropathic pain states. Science 290, 124–127.

Brack, A., Stein, C., 2003. The role of the peripheral nervous system in immune cell recruitment. Exp. Neurol. 184, 44–49.

Brück, W., 1997. The role of macrophages in Wallerian degeneration. Brain Pathol. 7, 741–752.

Chen, X.H., Meaney, D.F., Xu, B.N., Nonaka, M., McIntosh, T.K., Wolf, J.A., Saatman, K.E., Smith, D.H., 1999. Evolution of neurofilament subtype accumulation in axons following diffuse brain injury in the pig. J. Neuropathol. Exp. Neurol. 58, 588–596.
Chung, R.S., Staal, J.A., McCormack, G.H., Dickson, T.C., Cozens, M.A., Chuckowree, J.A., Quilty, M.C., Vickers, J.C., 2005. Mild axonal stretch injury in vitro induces a progressive series of neurofilament alterations ultimately leading to delayed axotomy. J. Neurotrauma 22, 1081–1091.
Colburn, R.W., DeLeo, J.A., Rickman, A.J., Yeager, M.P., Kwon, P., Hickey, W.F., 1997. Dissociation of microglial activation and neuropathic pain behaviors following peripheral nerve injury in the rat. J. Neuroimmunol. 79, 163–175.
Colburn, R.W., Rickman, A.J., DeLeo, J.A., 1999. The effect of site and type of nerve injury on spinal glial activation and neuropathic pain behavior. Exp. Neurol. 157, 289–304.
Côté, P., Cassidy, J., Carroll, L., 1998. The Saskatchewan health and back pain survey: the prevalence of neck pain and related disability in Saskatchewan adults. Spine 23, 1689–1698.
Côté, P., Cassidy, J.D., Carroll, L., 2000. The factors associated with neck pain and its related disability in the Saskatchewan population. Spine 25, 1109–1117.
Cuellar, J.M., Montesano, P.X., Carstens, E., 2004. Role of TNF-alpha in sensitization of nociceptive dorsal horn neurons induced by application of nucleus pulposus to L5 dorsal root ganglion in rats. Pain 110, 578–587.
Cui, J.G., Holmin, S., Mathiesen, T., Meyerson, B.A., Linderoth, B., 2000. Possible role of inflammatory mediators in tactile hypersensitivity in rat models of mononeuropathy. Pain 88, 239–248.
Freeman, M.D., Croft, A.C., Rossignol, A.M., Weaver, D.S., Reiser, M., 1999. A review and methodologic critique of the literature refuting whiplash syndrome. Spine 24, 86–96.
Hashizume, H., DeLeo, J.A., Colburn, R.W., Weinstein, J.N., 2000. Spinal glial activation and cytokine expression after lumbar root injury in the rat. Spine 25, 1206–1217.
Hubbard, R.D., Chen, Z., Winkelstein, B.A., 2008. Transient cervical nerve root compression modulates pain: load thresholds for allodynia and sustained changes in spinal neuropeptide expression. J. Biomech. 41, 677–685.
Iwata, A., Stys, P.K., Wolf, J.A., Chen, X.H., Taylor, A.G., Meaney, D.F., Smith, D.H., 2004. Traumatic axonal injury induces proteolytic cleavage of the voltage-gated sodium channels modulated by tetrodotoxin and protease inhibitors. J. Neurosci. 24, 4605–4613.
Kirita, T., Takebayashi, T., Mizuno, S., Takeuchi, H., Kobayashi, T., Fukao, M., Yamashita, T., Tohse, N., 2007. Electrophysiologic changes in dorsal root ganglion neurons and behavioral changes in a lumbar radiculopathy model. Spine 32, E65–72.
Kobayashi, S., Yoshizawa, H., 2002. Effect of mechanical compression on the vascular permeability of the dorsal root ganglion. J. Orthop. Res. 20, 730–739.
Kobayashi, S., Yoshizawa, H., Hachiya, Y., Ukai, T., Morita, T., 1993. Vasogenic edema induced by compression injury to the spinal nerve root. Distribution of intravenously injected protein tracers and gadolinium-enhanced magnetic resonance imaging. Spine 18, 1410–1424.
Kobayashi, S., Yoshizawa, H., Yamada, S., 2004. Pathology of lumbar nerve root compression. Part 2: morphological and immunohistochemical changes of dorsal root ganglion. J. Orthop. Res. 22, 180–188.
Lee, K.E., Thinnes, J.H., Gokhin, D.S., Winkelstein, B.A., 2004. A novel rodent neck pain model of facet-mediated behavioral hypersensitivity: implications for persistent pain and whiplash injury. J. Neurosci. Methods 137, 151–159.
Li, Y., Dorsi, M.J., Meyer, R.A., Belzberg, A.J., 2000. Mechanical hyperalgesia after an L5 spinal nerve lesion in the rat is not dependent on input from injured nerve fibers. Pain 85, 493–502.
Ma, W., Eisenach, J.C., 2003. Cyclooxygenase 2 in infiltrating inflammatory cells in injured nerve is universally up-regulated following various types of peripheral nerve injury. Neuroscience 121, 691–704.
Ma, C., Shu, Y., Zheng, Z., Chen, Y., Yao, H., Greenquist, K.W., White, F.A., LaMotte, R.H., 2003. Similar electrophysiological changes in axotomized and neighboring intact dorsal root ganglion neurons. J. Neurophysiol. 89, 1588–1602.
Myers, R.R., Heckman, H.M., Rodriguez, M., 1996. Reduced hyperalgesia in nerve-injured WLD mice: relationship to nerve fiber phagocytosis, axonal degeneration, and regeneration in normal mice. Exp. Neurol. 141, 94–101.
Nakamura, S., Myers, R.R., 1999. Myelinated afferents sprout into lamina II of L3–5 dorsal horn following chronic constriction nerve injury in rats. Brain Res. 818, 285–290.
Nakamura, S.I., Myers, R.R., 2000. Injury to dorsal root ganglia alters innervation of spinal cord dorsal horn lamina involved in nociception. Spine 25, 537–542.
Nuckley, D.J., Konodi, M.A., Raynak, G.C., Ching, R.P., Mirza, S.K., 2002. Neural space integrity of the lower cervical spine: effect of normal range of motion. Spine 27, 587–595.
Obata, K., Yamanaka, H., Fukuoka, T., Yi, D., Tokunaga, A., Hashimoto, N., Yoshikawa, H., Noguchi, K., 2003. Contribution of injured and uninjured dorsal root ganglion neurons to pain behavior and the changes in gene expression following chronic constriction injury of the sciatic nerve in rats. Pain 101, 65–77.
Olmarker, K., Rydevik, B., Holm, S., 1989. Edema formation in spinal nerve roots induced by experimental, graded compression. An experimental study on the pig cauda equina with special reference to differences in effects between rapid and slow onset of compression. Spine 14, 569–573.
Podhajsky, R.J., Sekiguchi, Y., Kikuchi, S., Myers, R.R., 2005. The histologic effects of pulsed and continuous radiofrequency lesions at 42 degrees C to rat dorsal root ganglion and sciatic nerve. Spine 30, 1008–1013.
Ramer, M.S., French, G.D., Bisby, M.A., 1997. Wallerian degeneration is required for both neuropathic pain and sympathetic sprouting into the DRG. Pain 72, 71–78.
Rothman, S.M., Kreider, R.A., Winkelstein, B.A., 2005. Spinal neuropeptide responses in persistent and transient pain following cervical nerve root injury. Spine 30, 2491–2496.
Rutkowski, M.D., Pahl, J.L., Sweitzer, S., van Rooijen, N., DeLeo, J.A., 2000. Limited role of macrophages in generation of nerve injury-induced mechanical allodynia. Physiol. Behav. 71, 225–235.
Scherer, S.S., Salzer, J., 2001. Axon–Schwann cell interactions in peripheral nerve degeneration and regeneration, In: Jessen, K.R., Richardson, W.D. (Eds.), Glial Cell Development, 2nd ed. Oxford Univ. Press, Oxford, pp. 299–330.
Sekiguchi, Y., Kikuchi, S., Myers, R.R., Campana, W.M., 2003. ISSLS prize winner: erythropoietin inhibits spinal neuronal apoptosis and pain following nerve root crush. Spine 28, 2577–2584.
Sekiguchi, M., Kikuchi, S., Myers, R.R., 2004. Experimental spinal stenosis: relationship between degree of cauda equina compression, neuropathology, and pain. Spine 29, 1105–1111.
Sheen, K., Chung, J.M., 1993. Signs of neuropathic pain depend on signals from injured nerve fibers in a rat model. Brain Res. 610, 62–68.
Singh, A., Lu, Y., Chen, C., Kallakuri, S., Cavanaugh, J., 2006. A new model of traumatic axonal injury to determine the effects of strain and displacement rates. Stapp Car Crash J. 50, 601–623.
Sommer, C., Kress, M., 2004. Recent findings on how proinflammatory cytokines cause pain: peripheral mechanisms in inflammatory and neuropathic hyperalgesia. Neurosci. Lett. 361, 184–187.
Song, X.J., Zhang, J.M., Hu, S.J., LaMotte, R.H., 2003. Somata of nerve-injured sensory neurons exhibit enhanced responses to inflammatory mediators. Pain 104, 701–709.
Stone, J.R., Okonkwo, D.O., Dialo, A.O., Rubin, D.G., Mutlu, L.K., Povlishock, J.T., Helm, G.A., 2004. Impaired axonal transport and altered axolemmal permeability occur in distinct populations of damaged axons following traumatic brain injury. Exp. Neurol. 190, 59–69.
Tan, Z.Y., Donnelly, D.F., LaMotte, R.H., 2006. Effects of a chronic compression of the dorsal root ganglion on voltage-gated Na+ and K+ currents in cutaneous afferent neurons. J Neurophysiol. 95, 1115–1123.
Watanabe, K., Konno, S., Sekiguchi, M., Sasaki, N., Honda, T., Kikuchi, S., 2007. Increase of 200-kDa neurofilament-immunoreactive afferents in the substantia gelatinosa in allodynic rats induced by compression of the dorsal root ganglion. Spine 32, 1265–1271.
Watkins, L.R., Maier, S.F., 2002. Beyond neurons: evidence that immune and glial cells contribute to pathological pain states. Physiol. Rev. 82, 981–1011.
Waxman, S.G., Cummins, T.R., Dib-Hajj, S., Fjell, J., Black, J.A., 1999. Sodium channels, excitability of primary sensory neurons, and the molecular basis of pain. Muscle Nerve 22, 1177–1187.
White, F.A., Sun, J., Waters, S.M., Ma, C., Ren, D., Ripsch, M., Steflik, J., Cortright, D.N., Lamotte, R.H., Miller, R.J., 2005. Excitatory monocyte chemoattractant protein-1 signaling is up-regulated in sensory neurons after chronic compression of the dorsal root ganglion. Proc. Natl. Acad. Sci. 102, 14092–14097.
Winkelstein, B.A., DeLeo, J.A., 2002. Nerve root injury severity differentially modulates spinal glial activation in a rat lumbar radiculopathy model: considerations for persistent pain. Brain Res. 29, 294–301.
Winkelstein, B.A., DeLeo, J.A., 2004. Mechanical thresholds for initiation and persistence of pain following nerve root injury: mechanical and chemical contributions and injury. J. Biomech. Eng. 126, 258–263.
Winkelstein, B.A., Rutkowski, M.D., Weinstein, J.N., DeLeo, J.A., 2001. Quantification of neural tissue injury in a rat radiculopathy model: comparison of local deformation, behavioral outcomes, and spinal cytokine mRNA for two surgeons. J. Neurosci. Methods 111, 49–57.
Winkelstein, B.A., Weinstein, J.N., DeLeo, J.A., 2002. The role of mechanical deformation in lumbar radiculopathy: an in vivo model. Spine 27, 27–33.
Xie, W.R., Deng, H., Li, H., Bowen, T.L., Strong, J.A., Zhang, J.M., 2006. Robust increase of cutaneous sensitivity, cytokine production and sympathetic sprouting in rats with localized inflammatory irritation of the spinal ganglia. Neuroscience 142, 809–822.
Zhang, X.F., Zhu, C.Z., Thimmapaya, R., Choi, W.S., Honore, P., Scott, V.E., Kroeger, P.E., Sullivan, J.P., Faltynek, C.R., Gopalakrishnan, M., Shieh, C.C., 2004. Differential action potentials and firing patterns in injured and uninjured small dorsal root ganglion neurons after nerve injury. Brain Res. 1009, 147–158.